



LAWRENCE
LIVERMORE
NATIONAL
LABORATORY

Radiographic Capabilities of the MERCURY Monte Carlo Code

M. S. McKinley, A. E. Schach von Wittenau

April 9, 2008

ICRS-11 & RPSD-2008
Pine Mountain, GA, United States
April 13, 2008 through April 18, 2008

Disclaimer

This document was prepared as an account of work sponsored by an agency of the United States government. Neither the United States government nor Lawrence Livermore National Security, LLC, nor any of their employees makes any warranty, expressed or implied, or assumes any legal liability or responsibility for the accuracy, completeness, or usefulness of any information, apparatus, product, or process disclosed, or represents that its use would not infringe privately owned rights. Reference herein to any specific commercial product, process, or service by trade name, trademark, manufacturer, or otherwise does not necessarily constitute or imply its endorsement, recommendation, or favoring by the United States government or Lawrence Livermore National Security, LLC. The views and opinions of authors expressed herein do not necessarily state or reflect those of the United States government or Lawrence Livermore National Security, LLC, and shall not be used for advertising or product endorsement purposes.

Radiographic Capabilities of the MERCURY Monte Carlo Code

M. Scott McKinley, Alexis E. Schach von Wittenau

Lawrence Livermore National Laboratory

L-95, P. O. Box 808

Livermore, CA 94551, USA

ICRS-11 & RPSD-2008

Callaway Gardens in Pine Mountain, Georgia, USA

April 13-18, 2008

Pages: 14

Tables: 2

Figures: 5

This document was prepared as an account of work sponsored by an agency of the United States government. Neither the United States government nor Lawrence Livermore National Security, LLC, nor any of their employees makes any warranty, expressed or implied, or assumes any legal liability or responsibility for the accuracy, completeness, or usefulness of any information, apparatus, product, or process disclosed, or represents that its use would not infringe privately owned rights. Reference herein to any specific commercial product, process, or service by trade name, trademark, manufacturer, or otherwise does not necessarily constitute or imply its endorsement, recommendation, or favoring by the United States government or Lawrence Livermore National Security, LLC. The views and opinions of authors expressed herein do not necessarily state or reflect those of the United States government or Lawrence Livermore National Security, LLC, and shall not be used for advertising or product endorsement purposes.

MERCURY is a modern, parallel, general-purpose Monte Carlo code being developed at the Lawrence Livermore National Laboratory. Recently, a radiographic capability has been added. MERCURY can create a source of diagnostic, virtual particles that are aimed at pixels in an image tally. This new feature is compared to the radiography code, HADES, for verification and timing. Comparisons for accuracy were made using the French Test Object and for timing were made by tracking through an unstructured mesh. In addition, self consistency tests were run in MERCURY for the British Test Object and scattering test problem. MERCURY and HADES were found to agree to the precision of the input data. HADES appears to run around eight times faster than the MERCURY in the timing study. Profiling the MERCURY code has turned up several differences in the algorithms which account for this. These differences will be addressed in a future release of MERCURY.

I. INTRODUCTION

MERCURY¹ is a modern Monte Carlo particle transport code developed at Lawrence Livermore National Laboratory (LLNL) that will replace the older codes TART² and COG³ as the next generation, general purpose radiation transport code at LLNL. MERCURY can transport neutrons, gamma rays and light charged particles through a 1-D spherical, 2-D R-Z or unstructured meshes, 3-D Cartesian or unstructured mesh and/or 3-D combinatorial geometry. Cross sections are treated as either multigroup or continuous energy. MERCURY can perform static and dynamic source calculations and k_{eff} and α eigenvalue calculations.

MERCURY has recently implemented ray-trace diagnostic particles for use in tally images and point detectors. These particles travel through the geometry without changing direction and their weight is attenuated by the total cross section. Radiography was identified as a new application for MERCURY that could take advantage of these ray-trace particles. The source routines in MERCURY were slightly modified in order to produce radiographs.

For comparison, MERCURY was compared to HADES⁴, a validated radiographics code that was also developed at LLNL. The accuracy of MERCURY's radiographic capability was first verified on the French Test Object (FTO)⁵. Next, an unstructured, cylindrical geometry test problem was run to compare runtimes between the two codes. Further tests were performed using MERCURY for the British Test Object (BTO)⁶ and a test problem for coherent and incoherent scatter⁷.

II. RADIOGRAPHIC TEST PROBLEMS

Radiographic simulations of the FTO were performed using HADES and MERCURY to verify the accuracy of MERCURY. The FTO is made from four nested spheres as detailed in Table I. The radiograph is configured with a source of 4 MeV gammas located 100 cm away from the FTO. The tally plane is an 80 cm by 80 cm plane comprised of 1,000 pixels and located 250 cm away from the FTO. The linear and logarithmic intensity radiographic images, which were generated by VisIt⁸, are shown in Figs. 1 and 2. The MERCURY and HADES simulations agreed to within numerical accuracy of the machine.

Timing comparisons of MERCURY and HADES were performed by tracking millions of ray-trace particles through an unstructured, cylindrical geometry mesh. On this problem, HADES ran about 8 times faster than MERCURY. After profiling MERCURY, these timing differences were attributed to: (a) the cross section look-up, which accounted for 40% of the runtime, and (b) running the problem with a mesh that is embedded in combinatorial geometry, which accounted for 34% of the runtime. These issues easily can be corrected with a moderate amount of work, and should speed up MERCURY about a factor of 4.

MERCURY was also used to perform a radiograph of the BTO. The BTO is a series of nested cylinders comprised of polystyrene, tungsten, aluminum, graphite and iron. The interesting feature of the BTO is that it has gaps between the upper and lower cylinders. The object of this test was to determine if MERCURY could resolve the gaps in a radiographic image. A partial specification for the BTO may be found in Fig. 3, where the cylindrical axis is along the Z direction. The materials for this problem are specified in Table II. The linear and logarithmic intensity radiographic images are shown in Figs. 4 and 5. In these figures, the gaps are well resolved and in the expected locations.

The final test in this study was to include scattering into the radiograph. A test problem⁷ developed to test MCNP's⁹ scattering radiographic capability was used for this purpose. The problem geometry involves launching particles towards two cylinders. In one version of this problem, the first cylinder is located 150 cm from the source and is made out of tungsten with an inner diameter 2 cm and an outer diameter of 8 cm. This cylinder is 5 cm in thickness. An aluminum cylinder is located an additional 200 cm

towards the image plane. It has a radius of 18 cm and a thickness of 2.5 cm. The tally plane is a total of 450 cm from the source, and is composed of 50 by 50 pixels covering 40 cm by 40 cm.

MERCURY's approach to modeling this problem is to launch both "standard" transport and "ray-trace" diagnostic particles toward the object. At each collision of a transport particle, a diagnostic particle is created. This diagnostic particle is created with a weight that is modified by the probability, over all reactions, that a particle could be produced with its velocity aligned in the direction of each pixel. A probability table is created at problem initialization based on discretizing angles over equally spaced cones.

The inclusion of scattering added a small contribution to the radiographic image. This conclusion was determined by reducing the density of the cylinders and comparing the modified image to an image generated solely by using transport particles. Future work on this problem will involve a direct comparison to MCNP's results for the various configurations for this problem.

II. CONCLUSIONS/FUTURE WORK

The MERCURY Monte Carlo code now has a new radiographic capability. This new feature has been compared to the HADES radiographic code with regard to both accuracy and speed. While matching HADES' results very well, MERCURY does run 8 times slower for some problems. Some obvious speed improvements have been identified such as caching cross sections and improving geometry look-ups when a mesh is embedded in combinatorial geometry. These changes should improve MERCURY's speed by about a factor of 4.

Additional verification and validation of the MERCURY radiographic capability need to be performed. The radiographic image from the BTO needs to be compared to results from HADES. In addition, MERCURY's results should be compared to the simulated radiographs produced from MCNP. Comparisons with MCNP will allow for a cross check on MERCURY's simulated radiographs that include scattering.

Since simulated radiographs are a new feature, they are currently not as user-friendly as they could be. When modeling the radiograph-with-scatter test problem, the user has to enter 2,500 locations for the diagnostic particles to travel towards. This process could be greatly simplified. In addition, separating out the direct line of sight image from the scattered contribution is currently not an easy task for a user. Effort is required to make this discrimination procedure easier for the user.

AUSPICES

This work performed under the auspices of the U.S. Department of Energy by Lawrence Livermore National Laboratory under Contract DE-AC52-07NA27344.

REFERENCES

1. Mercury Code Team, "Mercury Home Page", Lawrence Livermore National Laboratory, <http://nuclear.llnl.gov/mercury> (2006).
2. R. Cullen, "Red Cullen's Home Page", <http://home.comcast.net/~redcullen1/> (2006).
3. R. Buck, E. Lent, T. Wilcox and S. Hadjimarkos, "COG User's Manual: A Multiparticle Monte Carlo Transport Code (Fifth Edition)", Lawrence Livermore National Laboratory, Internal Report UCRL-TM-202590 (2002).
4. M. B. Aufderheide III, D. M. Slone and A. E. Schach von Wittenau, "HADES, a Radiographic Simulation Tool," *Review of Progress in Quantitative Nondestructive Evaluation*, AIP Conf. Proc. #557 (Am. Inst. Phys., Melville, NY), Vol. 20A, pp. 507-513.
5. G. S. Cunningham and C. Morris, "The Development of Flash Radiography," *Los Alamos Science*, Num. 28, pp. 76-91, (2003).
6. A. Heller, "Uncovering Hidden Defects with Neutrons", *Science & Technology Review*, Lawrence Livermore National Laboratory, May 5, pp. 4-11, (2001).
7. D. Flamig, "Test Problem for Coherent and Incoherent Scatter", Los Alamos National Laboratory, LA-UR-075124.
8. The VISIT Team, "VISIT: Software that Delivers Parallel Interactive Visualization", Lawrence Livermore National Laboratory, <http://www.llnl.gov/visit/> (2003).
9. X-5 Monte Carlo Team, "MCNP-A General Monte Carlo N-Particle Transport Code, Version 5," Los Alamos National Laboratory Report LA-UR-03-1987, April 24, (2003).

TABLE I. French Test Object Configuration

Material	Radius (cm)	Density (g/cm³)
Air	1	10 ⁻⁶
Tungsten	4.5	19.35
Copper	6.5	8.96
Polystyrene	22.5	0.5

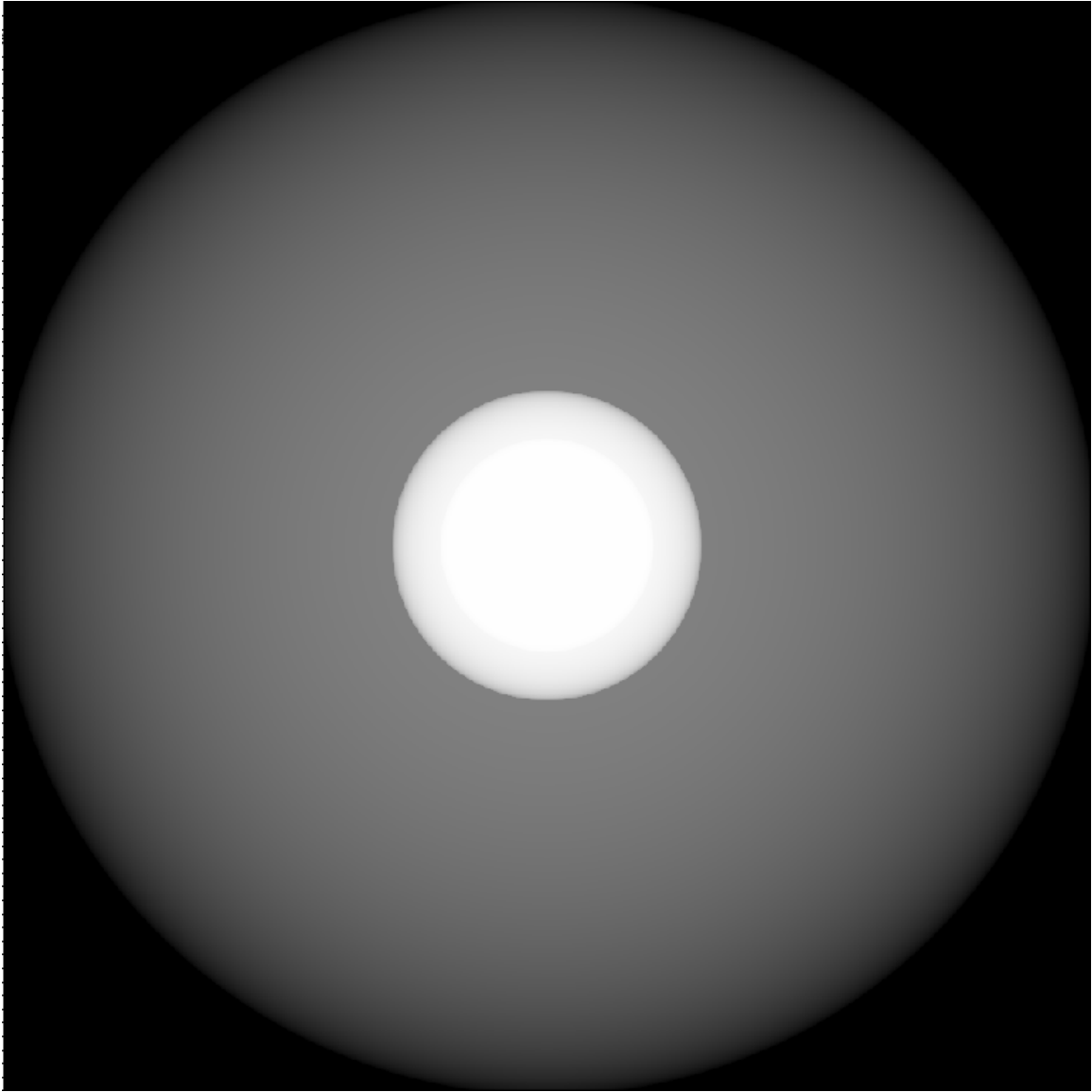


Fig. 1. Linear Intensity of the MERCURY FTO Radiograph

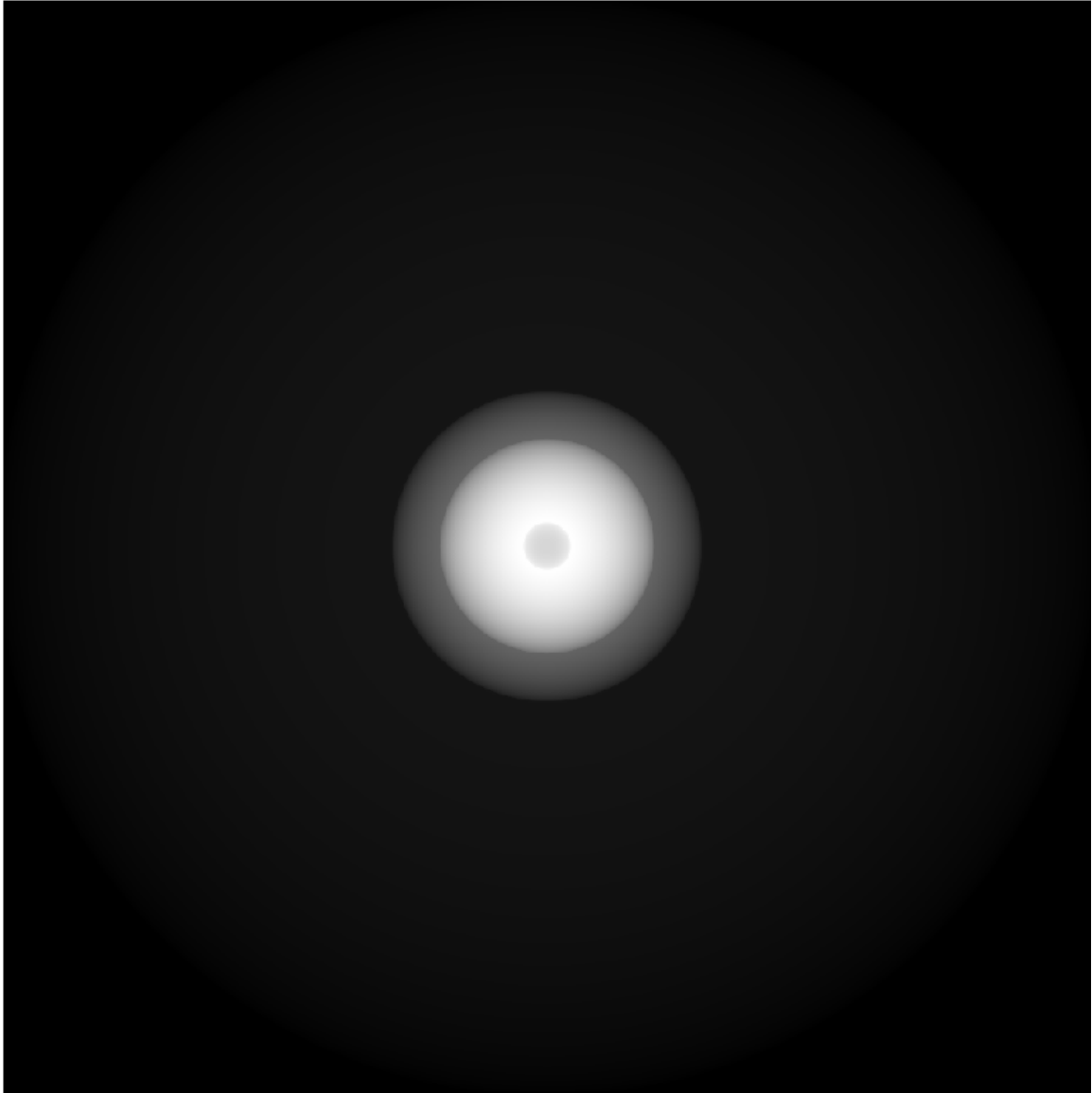


Fig. 2. Logarithmic Intensity of the MERCURY FTO Radiograph

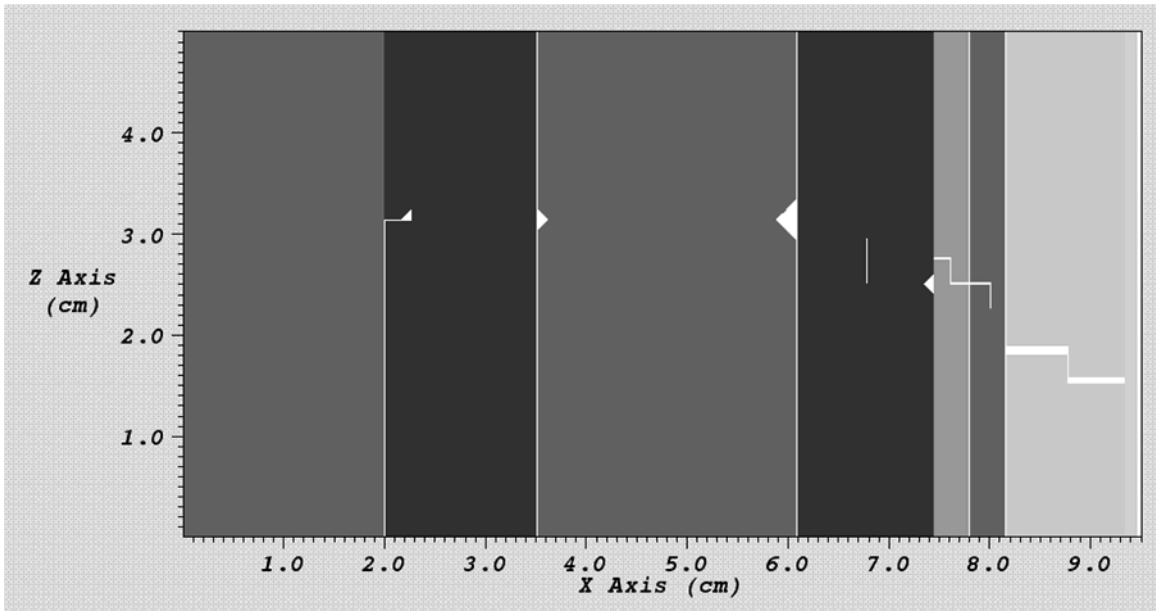


Fig. 3. Cutplane image of the nested cylinders in the British Test Object(BTO).

TABLE II. British Test Object(BTO) Configuration

Material	Approximate Radius (cm)	Density (g/cm³)
Polystyrene	2	0.84
Tungsten	3.5	18.5
Polystyrene	6.1	1.05
Tungsten	7.4	18.5
Aluminum	7.8	2.7
Polystyrene	8.2	0.735
Graphite	9.3	2.5
Iron	9.5	7.86

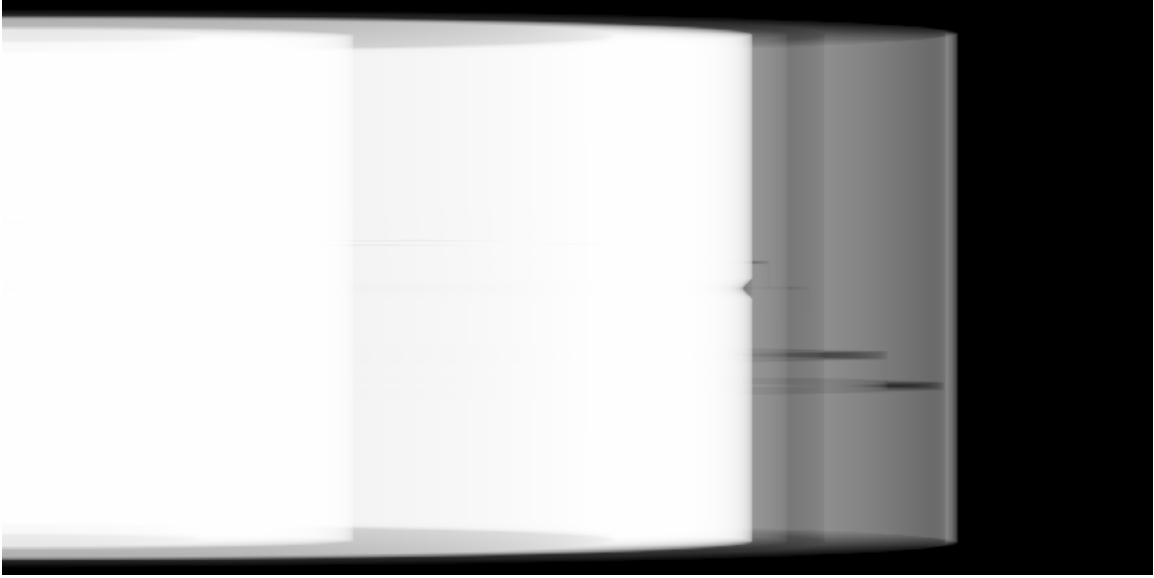


Fig. 4. Linear Intensity of the MERCURY BTO Radiograph

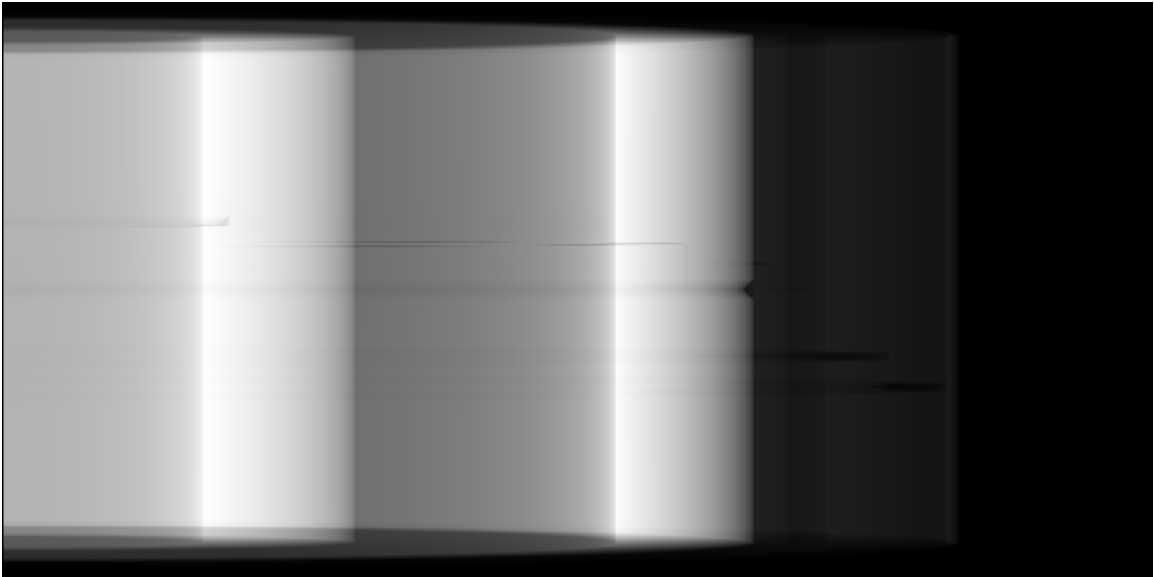


Fig. 5. Logarithmic Intensity of the MERCURY BTO Radiograph